Geochim. Brasil., 4(1): 59-83, 1990

EARLY AND LATE CRETACEOUS MAGMATISM FROM SÃO SEBASTIÃO ISLAND (SE - BRAZIL): GEOCHEMISTRY AND PETROLOGY

G. Bellieni[1], C.R. Montes-Lauar[2], A. De Min[3], E.M. Piccirillo[3], G. Cavazzini[4], A.J. Melfi[5], I.G. Pacca[5]

1. Dipartimento di Mineralogia e Petrologia, Università di Padova, Corso Garibaldi 37, 35100 Padova, Italy
2. Departamento de Geofísica, Instituto Astronômico e Geofísico da Universidade de São Paulo, Caixa Postal 9638, 01065 São Paulo, Brazil
3. Istituto di Mineralogia e Petrografia, Università di Trieste, Piazzale Europa 1, 34100 Trieste, Italy
4. Centro Studi Orogeno Alpi Orientali, c/o Dipartimento di Mineralogia e Petrologia, Università di Padova, Corso Garibaldi 37, 35100 Padova, Italy
5. Departamento de Geofísica, Instituto Astronômico e Geofísico da Universidade de São Paulo e Núcleo de Pesquisa em Geoquímica e Geofísica da Litosfera da USP, Caixa Postal 9638, 01065 São Paulo, Brazil

ABSTRACT

The São Sebastião island (236 km²), located along the coast of the São Paulo State (Southern Brazil), is characterized by precambrian granitic rocks affected by the Brasiliano tectonic-metamorphic cycle. This crystalline basement is intruded by Early Cretaceous (EC) subalkaline basic and acid dykes, as well as by Late Cretaceous (LC) alkaline stocks (syenites) and dykes (basanite to phonolite). EC and LC magmatic activities occurred, respectively, before and after the Africa-South America continental break-up and formation of the oceanic crust.

Geochemical, Sr-isotopic and mineral chemistry data point out that: (a) EC-dykes reveal a basic-acid bimodal character, similar to that of the "coeval" Paraná basin flood volcanics; the acid dykes correspond, in composition, to the acid volcanics of the northern Paraná basin; (b) the EC-dykes can represent the eastern extension of the inland Santos-Rio de Janeiro dyke swarm and (c) LC alkaline stocks and dykes constitute distinct groups, characterized by different Sr-isotope initial ratios (syenites: av. 0.7052 and basanites + tephrites = av. 0.7045), which indicate that they are related to different time-integrated mantle source materials.

RESUMO

A ilha de São Sebastião (área, 236 km²), localizada na costa norte do Estado de São Paulo, é constituída de rochas graníticas, afetadas pelo tectonismo e metamorfismo do Ciclo Brasiliano e intrudidas por diques básicos-ácidos subalcalinos do Cretáceo Inferior (EC), bem como por stocks (sienitos) e diques (basanitos e fonolitos) alcalinos do Cretáceo Superior (LC).

Os dois episódios vulcânicos, que ocorreram, respectivamente, antes e depois da fragmentação continental África-América do Sul e da formação da crosta oceânica, foram sistematicamente amostrados para os estudos geoquímicos e petrológicos.

Os estudos geoquímicos, isotópicos (Sr) e de química mineral conduziram às conclusões de que: a) os diques do Cretáceo Inferior apresentam caráter bimodal ácido-básico semelhante àquele encontrado para os derrames basálticos da bacia do Paraná; os diques ácidos correspondem em composição às vulcânicas ácidas da parte norte da bacia do Paraná; b) os dados sugerem, também, que os diques do Cretáceo Inferior representam a extensão leste do enxame de diques Santos-Rio de Janeiro; e c) os stocks e diques alcalinos do Cretáceo Superior constituem grupos distintos de rochas alcalinas caracterizados por valores diferentes de R_0 (média de 0,7052 para os sienitos e de 0,7045 para basanitos + tefritos), indicando que eles estão relacionados com materiais de fonte do manto com diferentes integrações no tempo.

INTRODUCTION

The São Sebastião island is located along the coast of the São Paulo State (Fig. 1) and its geology has never been studied in detail. The available geological and geochronological studies (Freitas, 1947; Hennies & Hasui, 1968, 1977) have only defined the general features of the Early and Late Cretaceous (EC and LC, respectively) magmatism.

The magmatic activity related to the opening of the South Atlantic ocean is concentrated towards the continental margin and it is essentially represented by the EC-flood volcanics and associated intrusives of the Paraná basin (Almeida, 1986; Melfi et al., 1988). Paleomagnetic results (Ernesto & Pacca, 1988; Ernesto et al., 1990), radiometric data (Melfi, 1967; Rocha-Campos et al., 1988) and bore-hole stratigraphy (Mantovani et al., 1988) show that the volcanic activity in the Paraná basin migrated from west to east and from south to north. Moreover, field research work and paleomagnetic data (Raposo & Ernesto, 1989) show that most of the Ponta Grossa dykes and probably those of the Santos-Rio de Janeiro coastline are younger than the Paraná stratoid basic and acid volcanics. These dyke swarms were emplaced during early stages of the major rifting processes responsible for crustal thinning and were probably magma feeders of volcanics, formed towards the continental margin of northern Paraná and

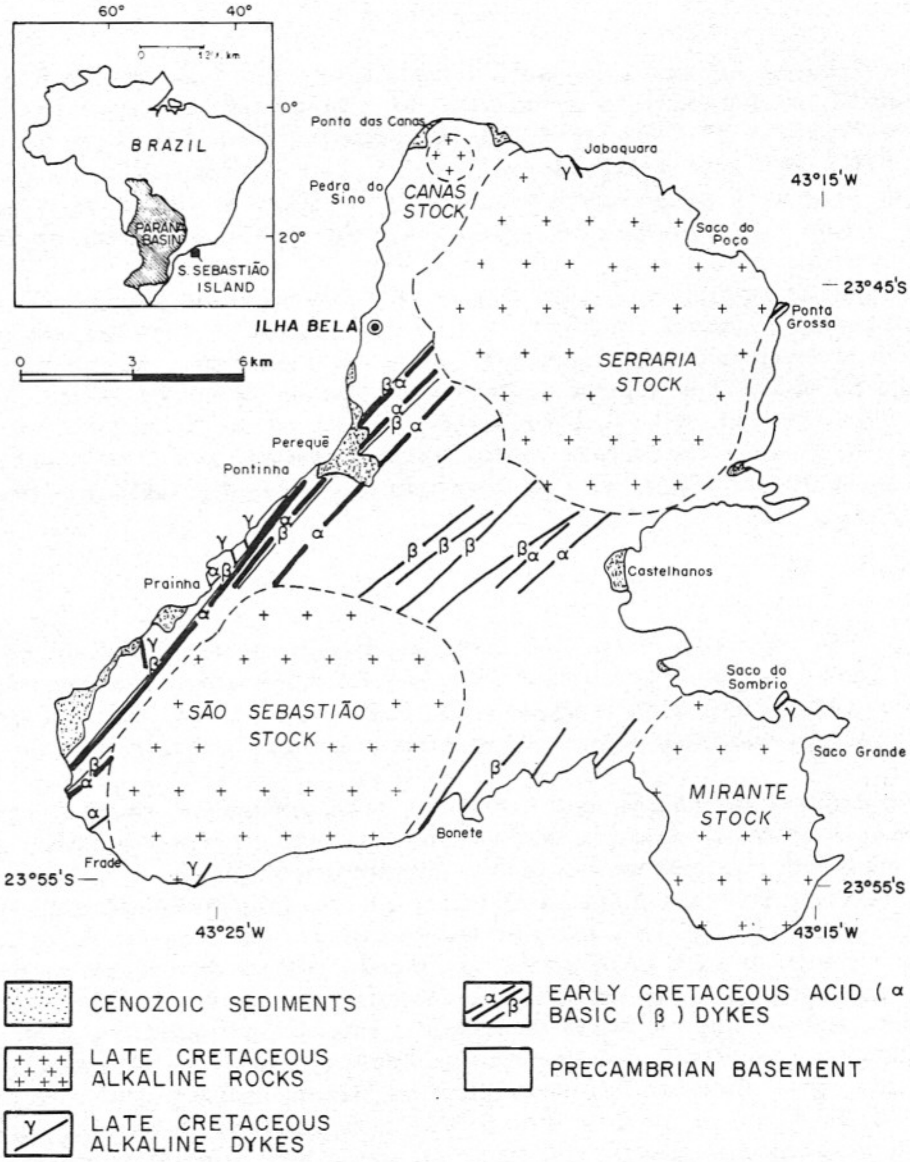

Figure 1 – Schematic geological map of the São Sebastião island. Modified from Hennies & Hasui (1977).

later eroded (Piccirillo et al., 1990). During the Late Cretaceous, when the Africa-S. America continental separation had already occurred, the inland magmatic activity of Brazil was alkaline and of the central type. This alkaline activity is mainly concentrated in northeastern Paraná, at the periphery of the basin. It follows that along the continental margin facing the northern Paraná, both the youngest EC-basalt magmatism, which preceded the continental break-up, and the alkaline magmatism, which occurred after the formation of the oceanic crust, can be found associated. These two distinct EC and LC types of magmatism, respectively, occur in the São Sebastião island.

The present paper mainly addresses to the geochemistry and petrology of the EC and LC magmatic activity of the São Sebastião island and its relationships with that outcropping inland, particularly the EC-dyke activity of Santos-Rio de Janeiro coastline.

GEOLOGY AND GEOCHRONOLOGY

The São Sebastião island is constituted by granitic rocks, modified by the tectonic and metamorphic Brasiliano Cycle and intruded by subalkaline basic-acid dykes, as well as alkaline stocks and dykes of Cretaceous age (Fig. 1).

The subalkaline basic and acid dykes have a NE trend, variable thickness (2-50 m) and extension (2-15 km). Whole-rock K-Ar age for an acid dyke is 122 ± 3 Ma (Amaral et al., 1966, age recalculated according to Steiger & Jaeger, 1977). Note that these dykes are cut by alkaline stocks.

The alkaline magmatism is represented by the Serraria, São Sebastião, Mirante and Canas (not considered in the present paper) stocks and dykes. Biotite K-Ar ages yielded values ranging from 81 ± 6 Ma to 87 ± 5 Ma with mean value of 84 ± 3 Ma (recalculated after Amaral et al., 1967; Hennies & Hasui, 1968). The alkaline dykes exhibit 0.5-3 m thickness, extension of few hundred meters and predominant NE direction. Their K-Ar age (78 ± 8 Ma to 83 ± 6 Ma) is similar to that of alkaline stocks, but they crosscut these intrusions. The alkaline dykes probably represent the youngest magmatic activity in the São Sebastião island.

CLASSIFICATION AND PETROGRAPHY

The EC basic dykes correspond to andesi-basalts, latibasalts and latiandesites, and the acid dykes to dacites and rhyodacites (Table 1, Fig. 2; De La Roche et al., 1980; Bellieni et al., 1981). The LC stocks plot in trachyte (syenite) field, while the dykes plot in the basanite, tephrite, phonolite, alkali basalt and quartz-trachyte fields (Fig. 2). In the AFM diagram (inset of Fig. 2), the EC-basalt dykes plot between the Hawaii alkaline and tholeiitic trends, while the LC-dykes fit the Hawaii alkaline trend. The Na_2O **vs.** K_2O diagram (inset of Fig. 2) shows that, in general, the alkaline rock types tend to have a potassic character.

The EC basic dykes are subaphyric or slightly porphyritic. Phenocrysts and/or microphenocrysts are mainly represented by abundant plagioclase laths, augite and minor Ti-magnetite. Ti-magnetite and ilmenite tend to be confined in groundmass. Common accessory is apatite, sometimes associated with biotite. Plagioclase may be partly replaced by epidote and chlorite; pyroxene occasionally show uralitic products. The EC acid dykes are characterized by plagioclase (up to 15 mm), augite, minor pigeonite and scarce Ti-magnetite phenocrysts. Apatites is a common accessory. The presence of chlorite, epidote in most basic and acid dykes indicates that these rocks suffered high-temperature alteration processes. To be noted that paleomagnetic results (Montes-Lauar & Pacca, in preparation) show that EC-dykes have been completely remagnetized by the Late Cretaceous syenitic stocks.

The LC syenitic stocks are holocrystalline and commonly have large phenocrysts of feldspar and pyroxene. Accessory minerals are biotite, amphibole, opaques, apatite and titanite; quartz and carbonate are also occasionally present. The LC basanites, tephrite and alkali basalt are usually porphyritic and show pyroxene phenocrysts set in a microcrystalline matrix. The only phonolitic dyke sample is subaphyric and characterized by scarce alkali feldspar, Ca-rich pyroxene, biotite microphenocrysts, and rare opaques and apatite set in a very fine groundmass. The quartz-trachytic dyke is holocrystalline and porphyritic. Phenocrysts and/or microphenocrysts are mainly represented by feldspar (sometimes pertite) and subordinately opaques and quartz. Groundmass is formed by alkali-feldspar dominant and biotite, amphibole, carbonate, opaques, quartz as accessory.

MINERAL CHEMISTRY

Microprobe analyses of phenocrysts and matrix phases were obtained for 14 representative samples of the São Sebastião magmatism. The analyses were carried out with a Cameca microprobe and are considered accurate to within 2-5% for major elements, and better than 10% for minor elements.

Average mineral compositions of early (phenocrysts and/or microphenocrysts and/or large grain cores) and late (grain rims) crystallization are given for pyroxenes, feldspars, Fe-Ti oxides and amphiboles in the Tables 2, 3, 4 and 5, respectively.

Pyroxenes

The *Early Cretaceous* andesi-basalts and latiandesites are characterized by Ca-rich pyroxenes (augites) which straddle the tholeiitic Skaergaard trend (Fig. 3). In general, late-crystallized augites have lower Ca and higher Fe contents than those of the early-crystallized augites. On the

Table 1. Major (% wt.) and trace (ppm) element contents for Early (1 to 15) and Late Cretaceous (16 to 35) magmatic rocks from São Sebastĩao island. Major element recalculated to 100% on a volatile-free basis. L.O.I. = loss on ignition; normative CIPW (Fe_2O_3/FeO = 0.15) parameters; Q = Quartz, Ne = Nepheline; (a) = original values; mg = atomic $Mg/Mg+Fe^{2+}$ (Fe_2O_3/FeO = 0.15); $^{87}Sr/^{86}Sr_m$ = present day value; R_o = initial (84 Ma) $^{87}Sr/^{86}Sr$ ratio; AB = andesi-basalt; LAND = latiandesite; DAC dacite; RD = rhyodacite; LB = latibasalt; LAT = latite; Q-TRC = quartz trachyte; AKB = alkali basalt; TRC = trachyte; BAS = basanite; TEPH tephrite; PHON = phonolite. S = stock; D = dyke; SERR = Serraria; SSEB = São Sebastião; MIR = Mirante. Sample SSG 3: CIPW-leucite = 11.86.

	1	2	3	4	5	6	7	8	9	10	11	12
SAMPLE	SS 39	SSA 56	SSA 57	SSA 59	SSA 62	SSA 63	SSA 64	SSA 65	SSA 66	SSA 67	SSA 68	SSA 69
	D	D	D	D	D	D	D	D	D	D	D	D
SiO_2	62.18	65.88	51.47	61.56	62.16	55.06	52.60	53.78	53.38	49.90	62.48	67.77
TiO_2	1.74	1.40	3.74	1.79	1.84	3.19	3.52	3.09	3.16	4.36	1.76	1.28
Al_2O_3	14.68	14.24	13.26	14.65	14.59	14.34	15.04	14.31	13.50	13.94	14.23	14.37
FeO_t	6.90	5.74	13.23	7.19	7.17	12.34	11.65	12.58	13.37	14.64	7.62	4.94
MnO	0.11	0.13	0.19	0.12	0.12	0.16	0.16	0.18	0.19	0.20	0.14	0.11
MgO	2.21	1.57	5.16	2.27	2.18	2.72	4.79	3.85	4.24	4.38	2.44	0.95
CaO	3.83	2.99	7.45	4.11	3.79	6.03	6.79	6.32	7.20	7.97	3.93	2.40
Na_2O	3.47	3.49	2.62	3.35	3.41	3.19	3.07	3.09	3.38	2.40	3.41	3.56
K_2O	4.14	4.12	2.31	4.18	4.02	2.21	1.64	2.09	1.16	1.41	3.55	4.22
P_2O_5	0.74	0.43	0.56	0.79	0.71	0.76	0.73	0.71	0.43	0.80	0.44	0.40
Fe_2O_3 (a)	1.40	1.56	4.80	1.51	2.14	3.33	2.51	3.11	5.49	4.46	2.16	0.77
FeO (a)	5.53	4.29	8.70	5.77	5.15	9.13	9.17	9.53	8.10	10.32	5.55	4.21
L.O.I. (a)	1.47	0.84	1.75	0.83	1.12	1.52	1.87	1.88	2.10	1.91	1.58	0.75
SUM (a)	99.97	100.22	100.63	100.22	100.07	100.17	100.20	100.19	100.21	100.24	100.10	100.03
Cr	2	1	22	1	1	17	21	8	10	61	9	1
Ni	6	3	47	9	5	33	49	32	37	51	21	7
Ba	1281	1109	498	1250	1288	726	575	658	451	470	968	1144
Rb	107	117	50	115	112	45	39	44	40	22	106	123
Sr	864	474	475	891	798	456	655	438	428	559	446	333
La	105	76	37	86	97	55	33	39	39	44	69	82
Ce	175	159	82	162	176	98	94	94	89	86	136	159
Nd	88	77	38	76	85	58	50	50	44	49	65	81
Zr	488	544	297	493	511	343	289	302	319	293	467	541
Y	48	54	42	48	51	54	44	48	49	47	51	64
Nb	57	54	32	57	60	33	29	30	33	31	46	51
R. TYPE	DAC	RD	AB	DAC	DAC	LAND	AB	LAND	AB	AB	DAC	RD
mg	0.393	0.357	0.441	0.390	0.380	0.308	0.454	0.382	0.391	0.377	0.393	0.280
Q	13.34	19.32	2.07	12.87	14.00	8.15	4.49	5.42	4.59	4.33	14.64	22.75
Ne	-	-	-	-	-	-	-	-	-	-	-	-
$^{87}Sr/^{86}Sr_m$	-	-	-	-	-	-	-	-	-	-	-	-
R_o (84 Ma)	-	-	-	-	-	-	-	-	-	-	-	-

Table 1 (cont.)

SAMPLE	13 SSG 7 D	14 SSG 8 D	15 SSG 9 D	16 SS 1 S SERR	17 SS 21 S SERR	18 SS 24 S SERR	19 SS 25 S SERR	20 SS 45 S SERR	21 SSA 55 S SERR	22 SSG 1 S SERR	23 SSG 6 S SERR	24 SS 13 S SSEB
SiO_2	65.59	51.97	58.91	63.34	63.53	63.99	63.49	66.93	64.93	62.15	54.65	65.38
TiO_2	1.36	3.25	1.29	0.97	0.91	0.78	0.89	0.60	0.75	0.92	1.76	0.57
Al_2O_3	15.36	15.77	18.30	17.21	17.14	16.65	16.88	16.83	16.87	18.49	18.59	16.83
FeO_t	5.49	12.05	5.90	4.07	3.66	4.33	3.78	2.47	3.79	4.08	6.20	3.56
MnO	0.12	0.16	0.18	0.11	0.15	0.19	0.15	0.07	0.23	0.15	0.19	0.13
MgO	1.21	4.50	2.28	0.90	0.89	0.88	0.87	0.33	0.50	0.85	2.24	0.38
CaO	3.11	6.26	3.63	1.45	1.77	0.93	1.75	0.39	0.98	2.09	5.31	1.15
Na_2O	3.11	3.56	3.86	5.17	5.23	5.44	5.16	5.94	5.86	4.82	4.65	5.42
K_2O	4.26	1.79	5.11	6.37	6.46	6.62	6.71	6.28	5.91	6.03	5.81	6.41
P_2O_5	0.40	0.69	0.55	0.41	0.27	0.19	0.30	0.15	0.18	0.41	0.61	0.17
Fe_2O_3 (a)	0.87	3.31	1.97	1.72	0.68	2.02	1.53	0.89	0.82	0.92	2.11	1.04
FeO (a)	4.64	8.76	3.94	2.48	2.99	2.46	2.35	1.65	3.01	3.21	4.22	2.59
L.O.I. (a)	1.07	2.48	3.07	0.95	1.65	1.08	1.41	0.64	1.10	0.97	1.05	0.70
SUM (a)	99.97	100.23	100.07	100.09	100.01	100.11	100.12	100.05	100.12	100.04	100.02	100.05
Cr	2	20	1	2	1	2	1	1	1	1	18	1
Ni	4	41	3	3	2	5	1	1	3	5	12	2
Ba	1186	585	1540	2610	380	601	435	48	8	1998	2562	426
Rb	114	67	129	90	74	161	70	106	91	84	138	93
Sr	483	557	644	215	41	107	41	10	7	220	1249	71
La	94	42	87	141	64	152	39	60	52	72	77	39
Ce	156	63	157	196	112	264	77	124	98	132	133	88
Nd	84	34	65	137	43	106	39	63	46	52	50	43
Zr	506	265	451	293	331	422	76	176	243	218	403	233
Y	52	40	38	154	28	59	21	26	33	32	34	28
Nb	51	26	98	73	63	184	31	53	73	73	126	53
R. TYPE	RD	LB	LAT	TRC	TRC	TRC	TRC	TRC	TRC	TRC	TAND	TRC
mg	0.309	0.430	0.439	0.309	0.328	0.291	0.318	0.214	0.209	0.296	0.422	0.179
Q	20.71	1.05	3.73	3.38	2.56	2.03	2.25	6.11	3.87	4.13	-	5.01
Ne	-	-	-	-	-	-	-	-	-	-	7.57	-
$^{87}Sr/^{86}Sr_m$	-	-	-	-	-	-	-	-	-	0.70655(2)	-	-
R_o (84 Ma)	-	-	-	-	-	-	-	-	-	0.70533	-	-

Table 1 (cont.)

SAMPLE	25 SS 18 S SEEB	26 SSG 4 S SSEB	27 SSG 5 S SSEB	28 SSG 10 S MIR	29 SS 8 D	30 SS 52 D	31 SSA 58 D	32 SSA 60 D	33 SSA 61 D	34 SSG 2 D	35 SSG 3 D
SiO_2	65.58	64.01	65.40	62.86	44.92	59.42	65.54	46.39	44.87	45.99	42.18
TiO_2	0.51	0.70	0.33	0.66	2.72	0.10	0.81	2.60	2.51	2.64	2.12
Al_2O_3	15.95	18.04	17.42	19.47	15.22	18.96	16.20	15.99	14.98	17.35	13.56
FeO_t	4.55	3.81	3.92	2.24	13.11	5.05	4.67	12.57	12.22	12.84	12.49
MnO	0.21	0.21	0.19	0.08	0.25	0.44	0.20	0.19	0.18	0.23	0.28
MgO	0.34	0.57	0.24	0.74	7.43	0.10	0.74	6.89	9.19	5.94	11.05
CaO	1.21	1.47	1.13	1.52	10.58	1.03	1.18	9.54	11.46	7.83	13.70
Na_2O	5.56	5.41	5.32	4.85	2.96	9.17	6.13	3.22	2.10	3.42	1.25
K_2O	5.98	5.55	5.96	7.40	2.03	5.69	4.30	2.25	2.14	3.02	2.64
P_2O_5	0.11	0.23	0.08	0.20	0.78	0.03	0.24	0.36	0.35	0.76	0.74
Fe_2O_3 (a)	1.09	1.23	1.22	0.47	6.17	1.59	3.24	6.23	5.10	5.83	5.40
FeO (a)	3.52	2.66	2.77	1.80	7.04	3.51	1.71	6.75	7.44	7.17	7.26
L.O.I. (a)	1.07	1.09	1.21	0.97	3.79	1.90	0.79	1.18	1.18	3.09	2.77
SUM (a)	100.09	100.07	100.07	100.01	100.42	99.80	100.35	100.12	100.11	100.41	100.35
Cr	2	1	1	1	30	1	1	85	270	12	293
Ni	3	4	3	1	48	3	5	55	116	34	178
Ba	218	1403	153	259	490	35	1093	780	590	855	544
Rb	103	76	106	120	56	611	103	51	45	81	112
Sr	36	207	27	119	1507	34	95	965	805	1218	918
La	28	41	30	50	65	324	118	40	32	71	54
Ce	66	92	62	104	96	501	204	69	60	111	115
Nd	36	45	43	47	44	186	85	31	26	48	50
Zr	112	178	235	192	348	2411	736	228	216	341	259
Y	33	29	28	20	35	125	67	26	25	36	34
Nb	64	56	45	43	106	459	140	59	54	110	60
R. TYPE	TRC	TRC	TRC	TRC	BAS	PHON	Q-TRC	BAS	AKB	TEPH	BAS
mg	1.333	0.231	0.111	0.399	0.534	0.039	0.242	0.526	0.603	0.484	0.641
Q	5.48	5.57	6.40	1.41	-	-	7.69	-	-	-	-
Ne	-	-	-	-	8.08	15.54	-	7.68	7.23	8.03	5.54
$^{87}Sr/^{86}Sr_m$	-	-	-	0.70855 (2)	-	-	-	-	-	0.70456 (3)	0.70504 (2)
R_o (84 Ma)	-	-	-	0.70507	-	-	-	-	-	0.70433	0.70462

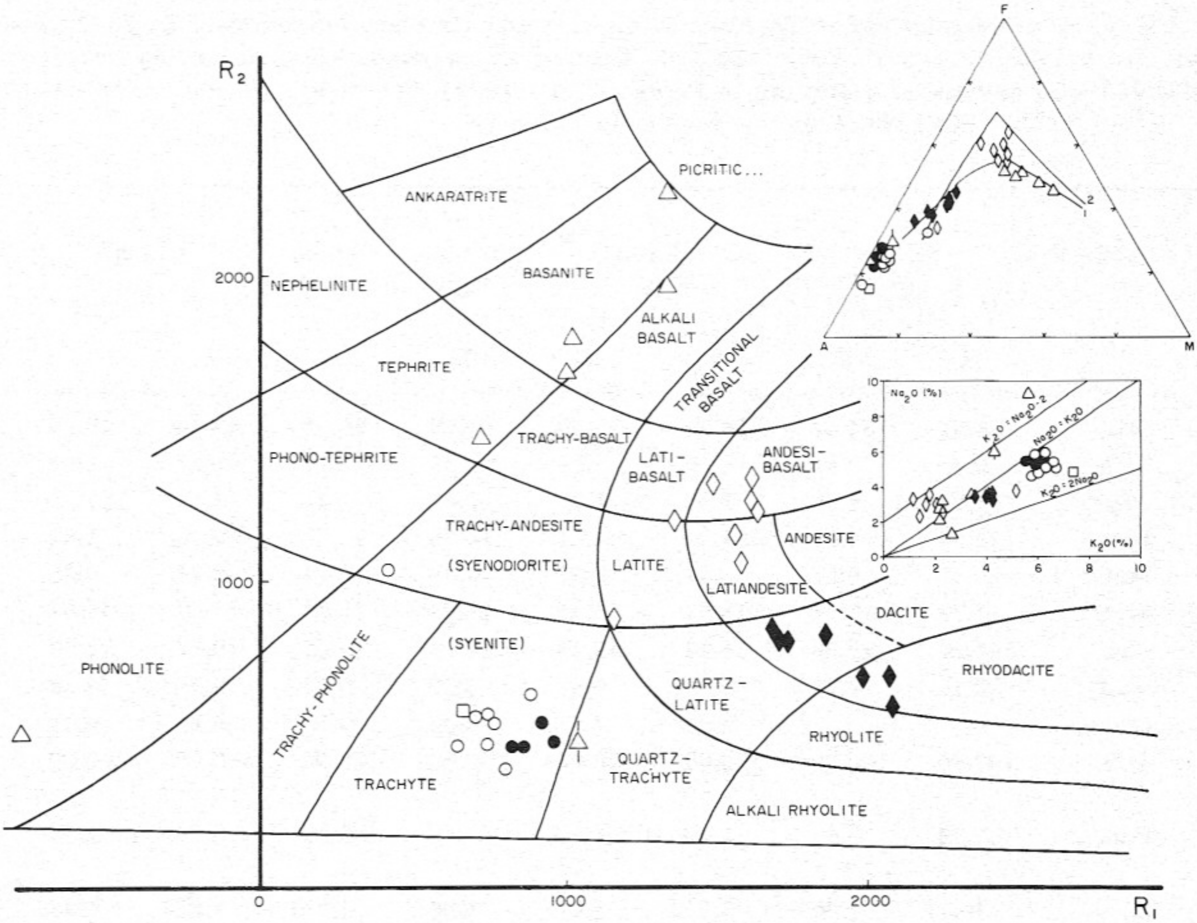

Figure 2 – Classificative R_1-R_2 diagram for the São Sebastião island magmatism (De La Roche et al., 1980; Bellieni et. al., 1981). Diamonds = Early Cretaceous dykes; triangles = Late Cretaceous dykes; circles = Serraria stock; solid circles = São Sebastião stock; square = Mirante stock and vertical bar triangle = dyke sample SSA 58. Insets: A (Na_2O + K_2O) - F (FeO_t) - M (MgO), and Na_2O **vs.** K_2O plots. 1 and 2 = alkaline and tholeiitic suites from Hawaii, respectively.

other hand, dacite and rhyodacite (DR) dykes contain both high and low-Ca (pigeonite) pyroxenes. DR-augites have compositions and elemental variations similar to those of the associated tholeiitic dykes and do not show a pronounced Fe-enrichment due to the concurrent crystallization of Ti-magnetite. Notably, EC-dykes of São Sebastião island have pyroxene compositions similar to those of high-TiO_2 tholeiitic dykes of Santos-Rio de Janeiro coastline, and of Chapecó acid flows and dykes from the northern Paraná basin (Comin-Chiaramonti et al., 1983; Bellieni et al., 1988).

The *Late Cretaceous* alkaline dykes (basanites) and stock (syenodiorite) are characterized by salites, while syenites contain salites, augites and Fe-augites (Fig. 4). Note that the Ca-rich pyroxene of the syenite SSG 5 has high (2.3% wt.) Na_2 content. The highest Fe-enrichment is found for the pyroxenes of the São Sebastião stock, which are somewhat more evolved than those of Serraria and Mirante analogues. Na-Mg-Fe** (Fe^{2+} + Mn + Fe^{3+} - Na) diagram (Fig. 4) reveals that the acmite content of pyroxenes from alkaline rock-types is generally low, excepting some pyroxenes from the São Sebastião syenites and the Serraria syenodiorite (SSG 6). The latter pyroxenes conform to the trend defined for the Piratini phonolite suite (Barbieri et al., 1987).

Feldspar

The *Early Cretaceous* andesi-basalts and latiandesites have plagioclase with anorthite content in the range 56-39% wt.,

Table 2. Average microprobe analyses of Ca-rich and Ca-poor pyroxenes of early (E) and late (L) crystallization for Early and Late Cretaceous magmatic rocks from São Sebastião island. Fe_2O_3 calculated according to Papike et al. (1974). Fe* = Fe^{2+} + Mn + Fe^{3+}; Fe** = Fe^{3+} + Fe^{2+} + Mn - Na. Abbreviations as in Table 1.

SAMPLE	1 SS 39 D		4 SSA 59 D		6 SSA 63 D	7 SSA 64 D	10 SSA 67 D	
	E	L	E	L	L	L	E	L
SiO_2	51.01	51.61	50.74	50.59	51.10	50.95	49.70	49.39
TiO_2	0.85	0.84	1.13	0.89	1.13	1.27	1.67	1.81
Al_2O_3	1.94	1.36	2.36	1.71	1.88	2.47	3.69	3.34
FeO_t	12.54	14.02	13.21	14.61	14.76	11.63	10.70	12.52
MnO	0.37	0.57	0.41	0.57	0.37	0.34	0.20	0.28
MgO	14.77	13.74	13.53	13.56	11.73	14.04	14.17	14.04
CaO	18.20	17.58	18.22	17.76	18.74	19.05	19.37	18.32
Na_2O	0.33	0.29	0.37	0.31	0.25	0.23	0.37	0.29
Cr_2O_3	-	-	0.03	-	0.02	0.02	0.13	0.01
SUM	100.00	100.00	100.00	100.00	100.00	100.00	100.00	100.00
Fe_2O_3	2.20	0.53	1.20	1.71	-	0.49	1.93	2.18
Si	1.911	1.949	1.912	1.916	1.944	1.911	1.856	1.855
Al^{IV}	0.086	0.051	0.088	0.076	0.056	0.089	0.144	0.145
SUM	1.996	2.000	2.000	1.992	2.000	2.000	2.000	2.000
Al^{VI}	-	0.010	0.016	-	0.028	0.020	0.018	0.003
Fe^{2+}	0.331	0.428	0.382	0.414	0.470	0.351	0.280	0.332
Fe^{3+}	0.062	0.015	0.034	0.049	-	0.014	0.054	0.061
Cr^{3+}	-	-	0.001	-	0.001	0.001	0.004	-
Mg	0.824	0.773	0.759	0.765	0.665	0.785	0.788	0.786
Mn	0.012	0.018	0.013	0.018	0.012	0.011	0.006	0.009
Ti	0.024	0.024	0.032	0.025	0.032	0.036	0.047	0.051
Ca	0.730	0.711	0.735	0.721	0.764	0.766	0.775	0.737
Na	0.024	0.021	0.027	0.023	0.019	0.017	0.027	0.021
SUM	2.007	2.000	1.999	2.015	1.991	2.001	1.999	2.000
Ca	37.27	36.56	38.22	36.65	39.98	39.75	40.72	38.29
Mg	42.06	39.74	39.47	38.89	34.80	40.74	41.41	40.83
Fe*	20.67	23.70	22.31	24.45	25.22	19.51	17.87	20.88
Na	-	-	-	-	-	-	-	-
Mg	-	-	-	-	-	-	-	-
Fe**	-	-	-	-	-	-	-	-
R. TYPE	DAC		DAC		LAND	AB	AB	

Table 2 (cont.)

SAMPLE	12 SSA 69 D				13 SSG 7 D			
	E	L	E	L	E	L	E	L
SiO_2	51.58	51.41	51.60	51.49	51.52	51.22	52.54	51.84
TiO_2	0.85	0.67	0.40	0.40	0.74	0.77	0.43	0.42
Al_2O_3	1.83	1.17	0.55	0.57	1.19	1.26	0.55	0.56
FeO_t	11.69	14.43	24.70	24.95	14.06	14.51	23.08	23.65
MnO	0.54	0.73	1.03	1.16	0.63	0.57	1.03	1.01
MgO	14.92	13.52	17.97	17.60	13.80	13.77	17.87	18.08
CaO	18.36	17.77	3.74	3.83	17.86	17.66	4.42	4.34
Na_2O	0.23	0.28	-	-	0.20	0.24	0.08	0.06
Cr_2O_3	-	0.02	0.01	-	-	-	-	0.04
SUM	100.00	100.00	100.00	100.00	100.00	100.00	100.00	100.00
Fe_2O_3	1.09	1.19	0.07	0.09	0.91	1.09	-	0.13
Si	1.929	1.946	1.970	1.970	1.947	1.939	1.991	1.974
Al^{IV}	0.071	0.052	0.025	0.026	0.053	0.056	0.009	0.024
SUM	2.000	1.998	1.995	1.996	2.000	1.995	2.000	1.998
Al^{VI}	0.010	-	-	-	-	-	0.016	-
Fe^{2+}	0.335	0.424	0.787	0.796	0.419	0.429	0.732	0.749
Fe^{3+}	0.031	0.034	0.002	0.003	0.026	0.030	-	0.004
Cr^{3+}	-	0.001	-	-	-	-	-	0.001
Mg	0.831	0.763	1.023	1.004	0.777	0.777	1.009	1.025
Mn	0.017	0.023	0.033	0.038	0.020	0.018	0.033	0.033
Ti	0.024	0.019	0.011	0.011	0.021	0.022	0.012	0.012
Ca	0.736	0.721	0.153	0.157	0.723	0.716	0.180	0.177
Na	0.017	0.020	-	-	0.014	0.018	0.006	0.004
SUM	2.001	2.005	2.009	2.009	2.000	2.011	1.988	2.005
Ca	37.74	36.69	7.66	7.86	36.80	36.35	9.21	8.90
Mg	42.62	38.83	51.20	50.25	39.54	39.44	51.64	51.56
Fe*	19.64	24.48	41.14	41.89	23.66	24.21	39.15	39.54
Na	-	-	-	-	-	-	-	-
Mg	-	-	-	-	-	-	-	-
Fe**	-	-	-	-	-	-	-	-
R. TYPE	RD				RD			

Table 2 (cont.)

SAMPLE	22 SSG 1 S SERR		23 SSG 6 S SERR	25 SS 18 S SSEB		27 SSG 5 S SSEB	28 SSG 10 S MIR	
	E	L	E	E	L	E	E	L
SiO_2	51.57	51.72	51.03	49.94	49.14	48.82	51.80	52.16
TiO_2	0.56	0.49	1.41	0.45	0.21	0.71	0.73	0.71
Al_2O_3	0.85	0.87	2.84	0.51	0.20	3.88	1.52	1.62
FeO_t	13.94	14.23	6.88	20.95	25.68	26.92	11.28	11.13
MnO	0.95	0.96	0.50	1.40	1.50	1.06	0.91	0.71
MgO	11.13	10.33	12.71	6.06	3.20	5.77	10.97	10.50
CaO	20.39	20.78	23.40	20.02	19.09	10.50	22.14	22.32
Na_2O	0.59	0.58	1.23	0.53	0.94	2.33	0.66	0.83
Cr_2O_3	0.02	0.04	-	0.04	0.04	-	-	0.01
SUM	100.00	100.00	100.00	100.00	100.00	99.99	100.00	100.00
Fe_2O_3	1.60	0.77	3.85	1.55	2.30	3.95	0.65	0.01
Si	1.964	1.977	1.890	1.974	1.983	1.920	1.960	1.974
Al^{IV}	0.036	0.023	0.110	0.024	0.009	0.080	0.040	0.026
SUM	2.000	2.000	2.000	1.998	1.992	2.000	2.000	2.000
Al^{VI}	0.002	0.016	0.014	-	-	0.099	0.028	0.046
Fe^{2+}	0.399	0.433	0.107	0.656	0.798	0.768	0.339	0.352
Fe^{3+}	0.045	0.022	0.106	0.037	0.069	0.117	0.018	-
Cr^{3+}	0.001	0.001	-	0.001	0.001	-	-	-
Mg	0.631	0.589	0.701	0.362	0.192	0.338	0.619	0.592
Mn	0.031	0.031	0.015	0.047	0.052	0.035	0.029	0.023
Ti	0.016	0.014	0.039	0.013	0.006	0.021	0.021	0.020
Ca	0.832	0.851	0.928	0.848	0.825	0.443	0.898	0.905
Na	0.044	0.043	0.089	0.041	0.073	0.178	0.048	0.061
SUM	2.001	2.000	1.999	2.005	2.015	2.000	2.000	2.000
Ca	42.93	44.19	49.97	43.49	42.61	26.04	47.19	48.34
Mg	32.56	30.58	37.75	18.56	9.92	19.87	32.53	31.62
Fe*	24.51	25.23	12.28	37.95	47.47	54.09	20.28	20.04
Na	3.98	4.00	9.58	3.72	6.57	14.15	4.78	6.31
Mg	57.05	54.79	75.46	32.85	17.28	26.87	61.59	61.22
Fe**	38.97	41.21	14.96	63.43	76.15	58.98	33.63	32.47
R. TYPE	TRC		TAND	TRC		TRC	TRC	

Table 2 (cont.)

SAMPLE	32 SSA 60 D		35 SSG 3 D
	E	L	E
SiO_2	50.02	49.14	47.11
TiO_2	1.45	1.58	1.84
Al_2O_3	4.18	4.57	7.73
FeO_t	7.58	8.96	7.17
MnO	0.24	0.48	0.15
MgO	14.10	12.35	12.70
CaO	21.90	22.48	22.79
Na_2O	0.49	0.44	0.45
Cr_2O_3	0.04	-	0.06
SUM	100.00	100.00	100.00
Fe_2O_3	2.42	2.39	3.64
Si	1.852	1.837	1.745
Al^{IV}	0.148	0.163	0.255
SUM	2.000	2.000	2.000
Al^{VI}	0.034	0.039	0.082
Fe^{2+}	0.168	0.213	0.121
Fe^{3+}	0.067	0.068	0.101
Cr^{3+}	0.001	-	0.002
Mg	0.778	0.688	0.701
Mn	0.007	0.015	0.005
Ti	0.040	0.044	0.051
Ca	0.869	0.901	0.904
Na	0.035	0.032	0.032
SUM	1.999	2.000	1.999
Ca	46.00	47.80	49.34
Mg	41.19	36.50	38.26
Fe*	12.81	15.70	12.40
Na	3.43	3.25	3.45
Mg	76.27	69.92	75.54
Fe**	20.29	26.83	21.01
R. TYPE	BAS		BAS

Table 3. Average microprobe analyses of feldspars of early (E) and late (L) crystallization for Early and Late Cretaceous magmatic rocks from São Sebastião island. Or = orthoclase; Ab = albite; An = anorthite. Abbreviations as in Table 1.

SAMPLE	1 SS 39 D		4 SSA 59 D		6 SSA 63 D	7 SSA 64 D	10 SSA 67 D	
	E	L	E	L	L	L	E	L
SiO_2	55.61	60.19	56.86	60.73	55.23	56.92	54.18	58.34
TiO_2	0.13	0.08	0.09	0.07	0.14	0.08	0.14	0.10
Al_2O_3	27.70	24.72	27.19	24.67	27.83	26.85	28.56	25.89
FeO_t	0.55	0.45	0.22	0.12	0.80	0.57	0.76	0.58
CaO	9.88	6.35	9.16	6.18	10.07	8.87	10.92	7.75
Na_2O	5.51	7.65	6.27	8.07	5.54	6.16	5.04	6.88
K_2O	0.62	0.56	0.21	0.16	0.39	0.55	0.40	0.46
SUM	100.00	100.00	100.00	100.00	100.00	100.00	100.00	100.00
Or (% wt.)	3.71	3.31	1.23	0.93	2.30	3.25	2.40	2.73
Ab (% wt.)	46.95	65.06	53.20	68.38	47.29	52.47	42.98	58.59
An (% wt.)	49.34	31.64	45.57	30.69	50.41	44.29	54.63	38.69
R. TYPE	DAC		DAC		LAND	AB	AB	

SAMPLE	12 SSA 69 D		13 SSG 7 D		22 SSG 1 S SERR		23 SSG 6 S SERR	
	E	L	E	L	E	L	E	L
SiO_2	57.05	58.32	57.11	59.50	59.18	59.57	61.67	66.38
TiO_2	0.11	0.04	0.08	0.07	-	-	0.05	0.02
Al_2O_3	26.69	26.30	26.71	25.13	25.82	25.50	23.93	20.38
FeO_t	0.63	0.09	0.52	0.54	0.03	0.05	0.20	0.22
CaO	8.71	8.09	8.72	6.85	7.49	7.14	5.33	1.32
Na_2O	6.18	6.85	6.12	7.36	7.30	7.41	8.54	9.51
K_2O	0.65	0.31	0.74	0.55	0.18	0.33	0.18	2.17
SUM	100.00	100.00	100.00	100.00	100.00	100.00	100.00	100.00
Or (% wt.)	3.84	1.85	4.41	3.25	1.09	1.93	1.07	12.83
Ab (% wt.)	52.64	57.97	52.10	62.58	61.75	62.65	72.43	80.59
An (% wt.)	43.52	40.18	43.49	34.17	37.17	35.42	26.50	6.58
R. TYPE	RD		RD		TRC		TAND	

Table 3 (cont.)

SAMPLE	25 SS 18 S SSEB		27 SSG 5 S SSEB		28 SSG 10 S MIR		32 SSA 60 D	35 SSG 3 D
	E	L	E	L	E	L	L	L
SiO_2	65.54	64.84	67.02	67.14	66.04	66.04	58.51	57.65
TiO_2	-	-	0.04	0.05	0.06	0.06	0.02	0.02
Al_2O_3	18.54	18.46	19.17	19.23	19.19	19.55	26.19	26.70
FeO_t	0.40	3.37	0.21	0.25	0.08	0.17	0.14	0.24
CaO	-	0.10	0.17	0.19	0.42	0.72	7.95	8.58
Na_2O	3.11	7.07	7.77	8.30	5.44	6.55	7.03	6.65
K_2O	12.41	6.16	5.62	4.84	8.77	6.91	0.16	0.16
SUM	100.00	100.00	100.00	100.00	100.00	100.00	100.00	100.00
Or (% wt.)	73.61	37.64	33.26	28.65	51.86	40.39	0.95	0.93
Ab (% wt.)	26.39	61.84	65.89	70.39	46.03	55.51	59.55	56.42
An (% wt.)	-	0.52	0.85	0.96	2.10	3.46	39.51	42.65
R. TYPE	TRC		TRC		TRC		BAS	BAS

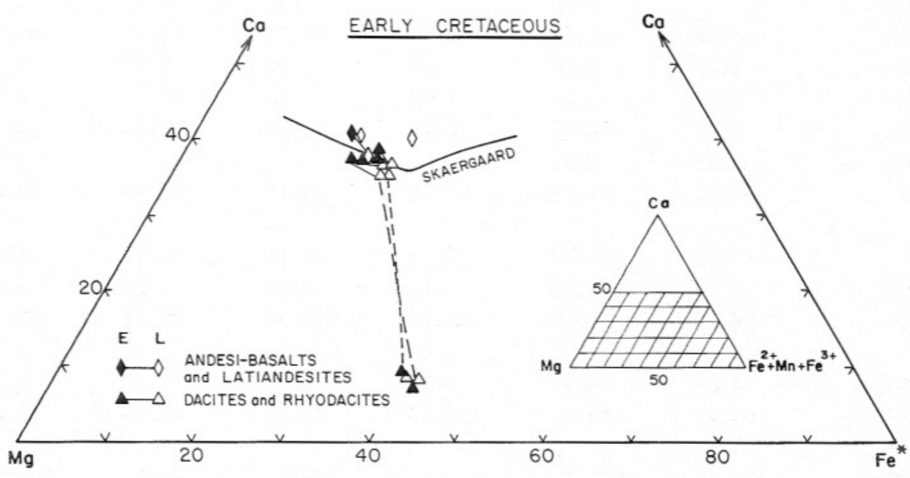

Figure 3 – Ca-Mg–Fe* (Fe^{2+} + Mn + Fe^{3+}) (atomic %) plot of pyroxenes from Early Cretaceous basic and acid dykes of São Sebastião island, compared with Skaergaard tholeiitic trend. E and L = early and late crystallizations, respectively.

while that of dacites and rhyodacites spans from 49 to 31% (Table 3, Fig. 5).

The *Late Cretaceous* basanites and syenites have andesitic plagioclase (An = 43-40 and 37-35% wt., respectively). Syenites are also characterized by alkali feldspars, whose orthoclase content (74-29% wt.) decreases in those of late crystallization (Fig. 5). The Serraria syenodiorite (SSG 6) is characterized by oligoclase (An = 26% wt.) and alkali feldspar (Or = 13% wt.).

Table 4. Average microprobe analyses for homogeneous late-crystallized magnetites and ilmenites from Early and Late Cretaceous magmatic rocks of São Sebastião island. Fe_2O_3 calculated according to Carmichael (1967). Abbreviations as in Table 1.

SAMPLE	1 SS 39 D	4 SSA 59 D	7 SSA 64 D	10 SSA 67 D	12 SSA 69 D	22 SSG 1 S SERR
			Ti-MAGNETITE			
SiO_2	0.25	0.13	0.26	0.26	0.15	0.19
TiO_2	24.38	17.90	19.52	7.76	15.87	3.46
Al_2O_3	1.46	0.08	1.14	0.41	0.61	0.21
FeO_t	68.52	78.93	75.47	88.01	80.48	93.67
MnO	1.58	0.63	0.77	0.26	0.68	0.31
MgO	1.08	0.07	0.42	0.03	0.03	0.05
CaO	0.58	-	0.19	0.15	0.04	-
Cr_2O_3	0.04	0.10	0.06	0.81	0.03	-
SUM	97.89	97.84	97.83	97.69	97.89	97.88
			ULVOSPINEL BASIS			
FeO	50.33	47.53	48.34	39.16	45.86	35.49
Fe_2O_3	20.21	34.88	30.15	54.27	38.45	64.64
SUM	99.91	101.34	100.84	103.11	101.73	104.34
			ILMENITES			
SiO_2	0.18	0.12	0.06	0.25	0.07	0.13
TiO_2	49.01	49.33	47.97	47.41	50.26	48.67
Al_2O_3	-	0.01	-	0.64	-	-
FeO_t	46.04	45.61	48.52	47.22	45.61	47.86
MnO	2.48	2.70	1.60	1.60	2.31	1.65
MgO	0.01	0.03	0.03	0.33	0.03	0.06
CaO	0.02	0.01	0.16	0.29	0.13	0.12
Cr_2O_3	0.03	0.01	-	-	-	-
SUM	97.77	97.82	98.34	97.75	98.39	98.48
FeO	41.73	41.70	41.33	40.35	42.72	41.98
Fe_2O_3	4.79	4.35	7.99	7.64	3.21	6.53
SUM	98.25	98.25	99.14	98.51	98.71	99.13
% R_2O_3	4.67	4.24	7.68	8.35	3.09	6.27
% Ulvosp.	69.42	50.76	55.83	22.66	45.09	10.24
T (^oC)	945.4	818.3	933.2	707.7	741.8	594.5
$-logfO_2$	12.3	14.8	12.0	16.2	17.0	19.7
R. TYPE	DAC	DAC	AB	AB	RD	TRC

Fe-Ti oxides

Magnetite occurs as phenocrysts and microphenocrysts. In the tholeiitic dykes magnetite is mainly confined to the groundmass. Ilmenite is comparatively scarce and usually occurs as thin elongated laths. Average compositions of homogeneous magnetite-ilmenite pairs of late crystallization are listed in Table 4.

Table 5. Average microprobe analyses for early (E) and late (L) crystallized amphiboles from Late Cretaceous syenitic intrusions of São Sebastião island. Structural formulae calculated on the basis of 23 atoms of O; Fe_2O_3 calculated according Papike et al. (1974). Abbreviations as in Table 1.

SAMPLE	23 SSG 6 S SERR	25 SS 18 S SSEB		27 SSG 5 S SSEB	
	L	E	L	E	L
SiO_2	39.38	47.77	48.00	46.44	46.03
TiO_2	3.48	1.43	1.19	1.11	1.15
Al_2O_3	11.72	2.81	2.61	3.16	3.09
FeO_t	20.41	31.75	32.91	34.38	33.00
MnO	0.75	1.11	1.10	1.34	1.50
MgO	7.89	3.19	2.78	1.63	1.65
CaO	11.45	7.17	7.77	7.52	7.87
Na_2O	2.13	3.53	2.70	2.85	2.87
K_2O	1.76	0.71	0.76	0.78	0.74
SUM	98.97	100.01	99.82	99.21	97.90
Fe_2O_3	1.64	-	0.56	0.61	0.73
Si	6.028	7.472	7.529	7.417	7.427
Al^{IV}	1.972	0.518	0.471	0.583	0.573
SUM	8.000	7.990	8.000	8.000	8.000
Al^{VI}	0.143	-	0.011	0.012	0.015
Fe^{2+}	2.424	4.153	4.251	4.519	4.365
Fe^{3+}	0.188	-	0.066	0.074	0.088
Mg	1.800	0.744	0.650	0.338	0.397
Mn	0.097	0.147	0.146	0.181	0.205
Ti	0.401	0.168	0.140	0.133	0.140
SUM	5.053	5.212	5.264	5.307	5.210
Ca	1.878	1.292	1.306	1.287	1.361
Na	0.632	1.075	0.973	0.883	0.898
K	0.344	0.142	0.152	0.159	0.152
SUM	2.854	2.409	2.431	2.329	2.411
R. TYPE	TAND	TRC		TRC	

Temperatures and fO_2 values (Buddington & Lindsley, 1964) fit the curves of NNO and QFM buffers (Fig. 6). The highest closure temperature (930 and 945°C), is found for dykes (andesi-basalt and dacite, respectively), while the lowest one (594°C) refers to a syenite sample of the Serraria stock.

Amphiboles

Amphibole is present in the syenitic intrusions (mainly São Sebastião and Serraria), where it also replaces pyroxene (e.g. SSG 6). Compositionally (Table 5), amphibole from syenites is of Fe-edenitic type, while that substituting pyroxene (Serraria syenodiorite) corresponds to Fe-pargasite (Leake, 1978).

GEOCHEMISTRY AND Sr-ISOTOPE DATA

Bulk-rock compositions (Table 1)

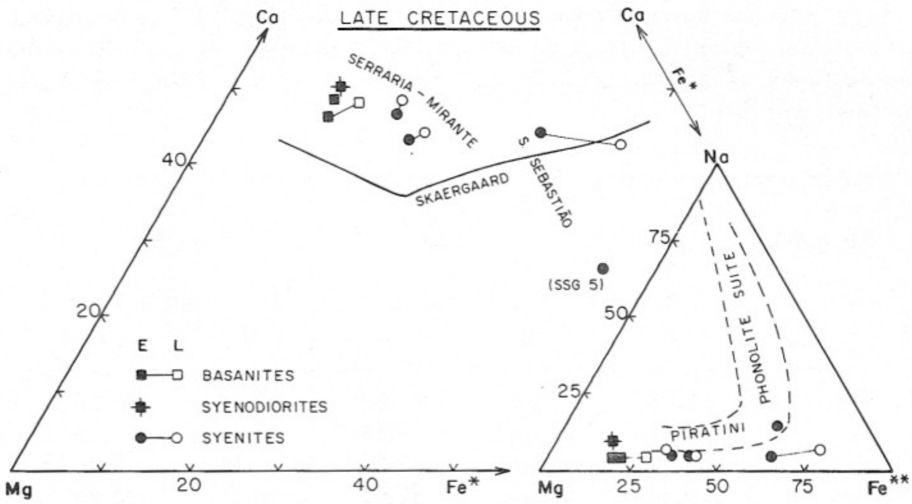

Figure 4 – Ca-Mg-Fe* (Fe^{2+} + Mn + Fe^{3+}) and Na-Mg-Fe** (Fe^{2+} + Mn + Fe^{3+}-Na) (atomic %) plots of pyroxenes from Late Cretaceous alkaline dykes (basanites) and intrusions (syenites and syenodiorite) of São Sebastião island. Skaergaard tholeiitic trend and Piratini phonolite suite are shown for comparison. E and L = early and late crystallizations, respectively.

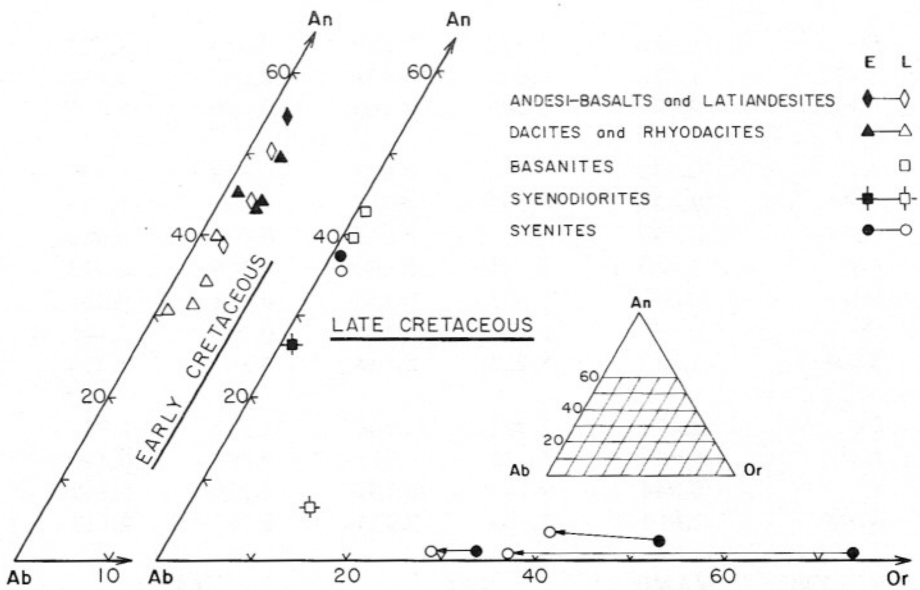

Figure 5 – Anorthite (An) - Albite (Ab) - Orthoclase (Or) (% wt.) plot of feldspars from Early and Late Cretaceous dykes and intrusions of São Sebastião island. E and L = early and late crystallizations, respectively.

were determined following the procedure described in Bellieni et al. (1983). Major element contents are considered accurate to within 2-5%, and trace element accuracy is better than 10%. Rare earth elements were measured by ICP spectrometry at Nancy University.

Sr-isotope ratios (Table 1) were determined according to the method described in Petrini et al. (1987). NBS-987 Sr standard analyses (Padova University) gave average values of 0.71027. Standard deviations of the isotopic ratios are expressed as 2 sigma of the mean value. Sr blank values are less than 2 ng.

The *Early Cretaceous* tholeiitic dykes

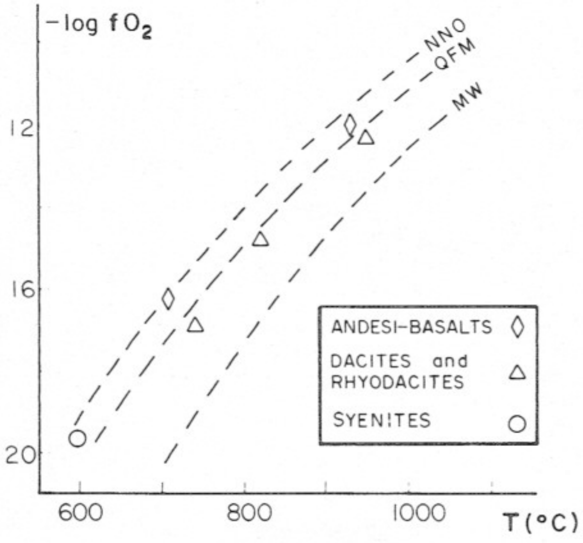

Figure 6 - T(°C) **vs.** -log fO_2 for Ti-magnetites and ilmenites of Early Cretaceous dykes (andesi-basalts, dacites and rhyodacites) and Late Cretaceous intrusion (syenite) from São Sebastião island. NNO: nickel-nickel-oxide, QFM: quartz-fayalite-magnetite, and MW: magnetite-wustite.

are somewhat evolved having mg values (at. Mg/Mg + Fe^{2+}, Fe_2O_3/FeO = 0.15) ranging from 0.45 to 0.31. These rock-type are high in TiO_2 (3.1-4.4% wt.) and incompatible elements (e.g. Zr = 293-343, Ba = 451-726, La = 33-55 ppm). The dacitic-rhyodacitic dykes are characterized by SiO_2 higher than 62% wt. and high incompatible element contents (e.g. Zr = 467-544, Ba = 968-1288, La = 69-105 ppm). Only one sample (SSG 9) has a SiO_2 content (59% wt.) intermediate between basic (50-55% wt.) and acid (62-68% wt.) dykes. It follows that the EC-magmatism of the São Sebastião island is virtually bimodal. The variation diagrams for major and trace elements **vs.** mg values (Fig. 7) and Zr (Fig. 8) show that basic and acid dykes are very similar in composition to the coeval basic and acid dykes from Santos-Rio de Janeiro coastline, except for La. Note that the acid dykes chemically correspond to the stratoid acid volcanics enriched in incompatible elements (Chapecó type) of northern Paraná basin (Bellieni et al., 1986; Piccirillo et al., 1988). Variation diagrams (Figs. 7, 8) show that acid dykes cannot be derived from the basic analogues by fractional crystallization. REE patterns (Fig. 9, Table 6) show that basic to acid dykes are somewhat fractionated (La_N/Yb_N: basic = av. 9.7 $\pm$ 0.3 and acid = av. 17.0 $\pm$ 3.9), showing distinct negative Eu-anomaly (Eu/Eu*: basic = av. 0.92 $\pm$ 0.04 and acid = av. 0.85 $\pm$ 0.09). In general, REE patterns of the EC-magmatism are similar to those of the corresponding rock-types from northern Paraná basin (Marques, 1988; Piccirillo et al., 1988; Marques et al., 1989).

The *Late Cretaceous* syenitic stocks are characterized, for decreasing mg value (Fig. 7), by increase in SiO_2, and decrease in TiO_2 (FeO_t), P_2O_5 (CaO), Ba, La, Sr and Zr, while K_2O, Rb, Nb and Y remain virtually constant. In general, these chemical variations indicate an important role of the accessory phases (e.g. apatite, titanite, opaques) in association with feldspars and Ca-rich pyroxene, in controlling magmatic evolution (cf. Fig. 8). This can explain the lower chondrite-normalized La/Yb ratios (Fig. 9, Table 6) of the more evolved São Sebastião stock (12.1- 12.2), relative to those of Serraria and Mirante stocks (23.7 and 26.6, respectively). Note that the latter syenitic stocks are characterized by a positive Eu-anomaly (Eu/Eu* = 1.11-1.52; "cumulus" feldspars), while that of São Sebastião stock has a negative Eu-anomaly (Eu/Eu* = 0.79-0.81). The LC basanite-peralkaline phonolite dykes are chemically distinct from the syenitic stocks (Figs. 7, 8). In terms of REE (Table 6), they are characterized by La_N/Yb_N, ranging from 21 (basanite and tephrite) to 18 (phonolite). The phonolite dyke shows a strong negative Eu-anomaly (Eu/Eu* = 0.10). The quartz-trachytic dyke (SSA 58) is similar in composition to the syenitic stocks, excepting for its higher Zr content (736 **vs.** 76-422 ppm).

$^{87}Sr/^{86}Sr$ initial (84 Ma) ratios (R_o) are available only for Late Cretaceous magmatism of São Sebastião island. Serraria and Mirante syenitic stocks have similar R_o values (0.70533 and 0.70507, respectively). These values are distinct from those of the alkaline dykes: basanite = 0.70462 and tephrite = 0.70433. On the whole, the LC-alkaline magmatism has R_o values similar to or higher than that of the Bulk Earth (R_o = 0.7045).

CONCLUDING REMARKS

An important feature shown by the

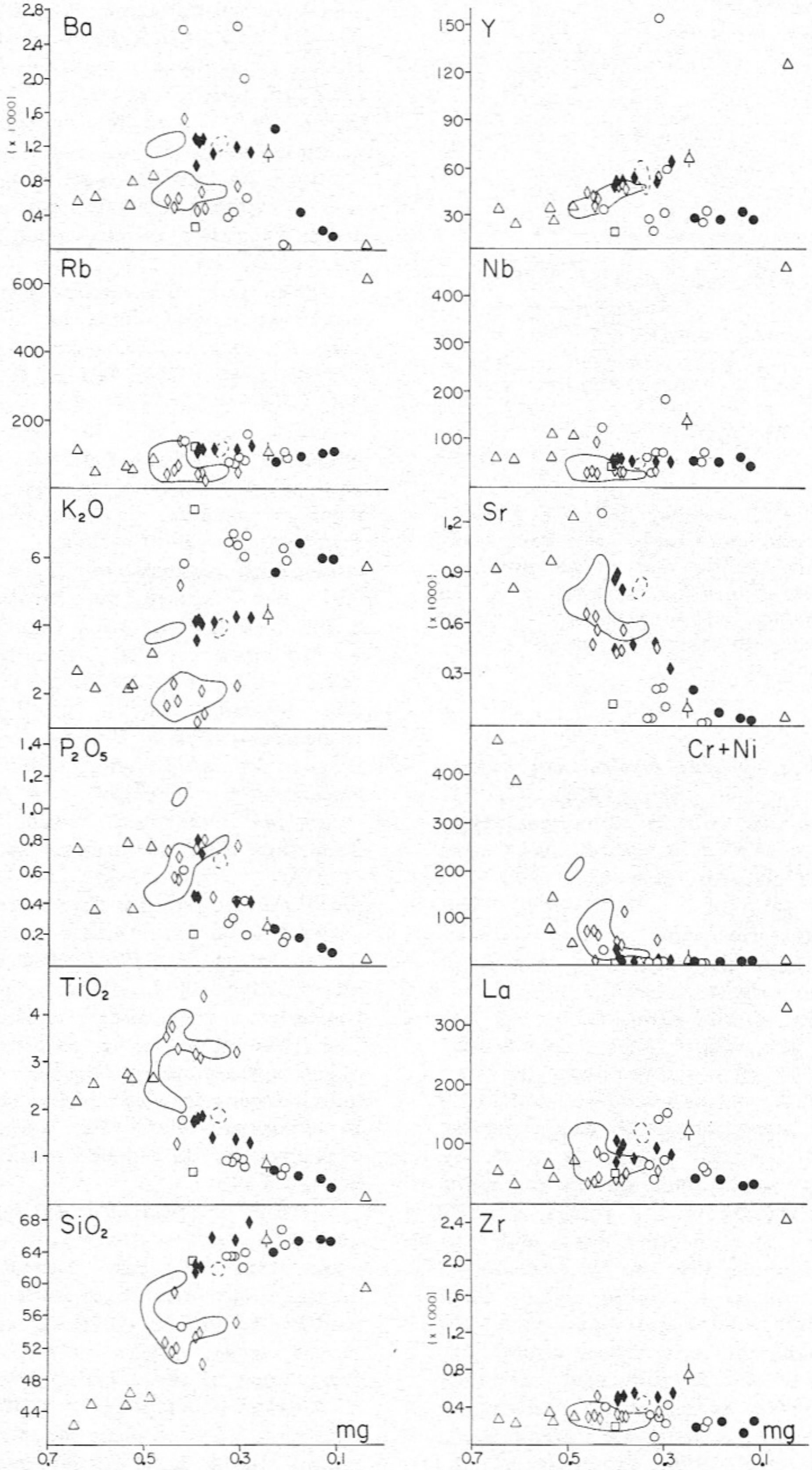

Figure 7 – Major (% wt.) and trace (ppm) elements vs. mg value (at. $Mg/Mg + Fe^{2+}$; Fe_2O_3/FeO = 0.15) for the Early and Late Cretaceous magmatism from the São Sebastião island. Symbols as in Figure 2; solid and dotted fields = basic and acid dykes, respectively, from Santos-Rio de Janeiro coastline.

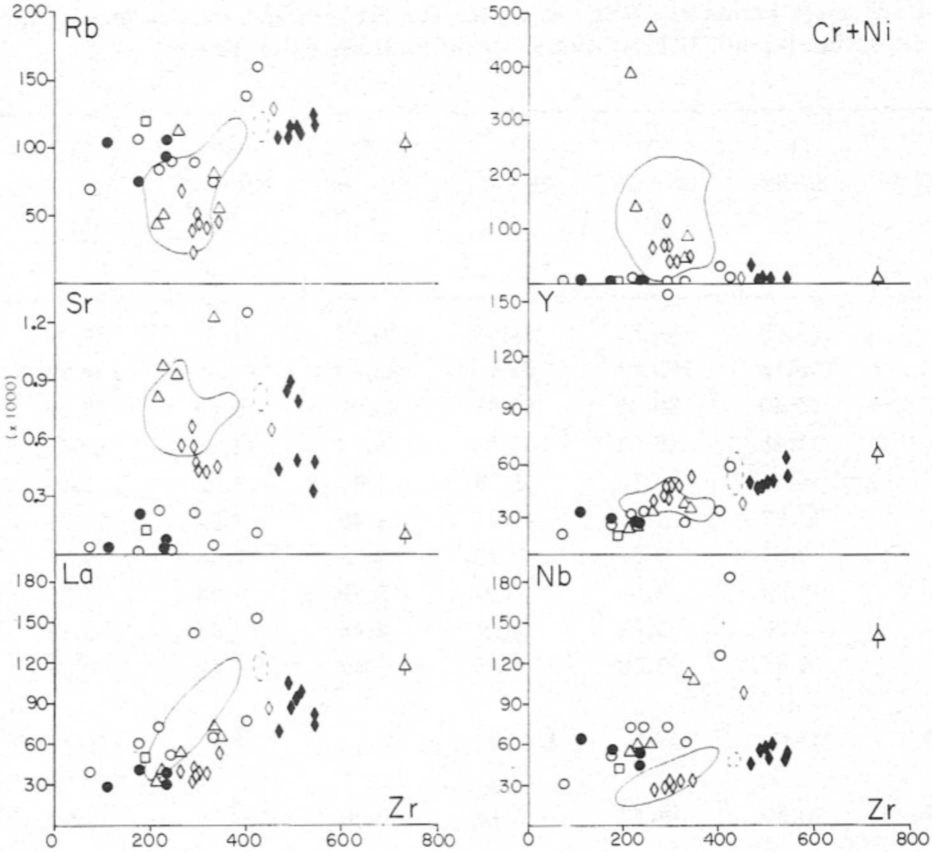

Figure 8 - Zr vs. Rb, Sr, La, Cr+Ni, Y and Nb (ppm) plots for the Early and Late Cretaceous magmatism from the São Sebastião island. Symbols as in Figures 2 and 7.

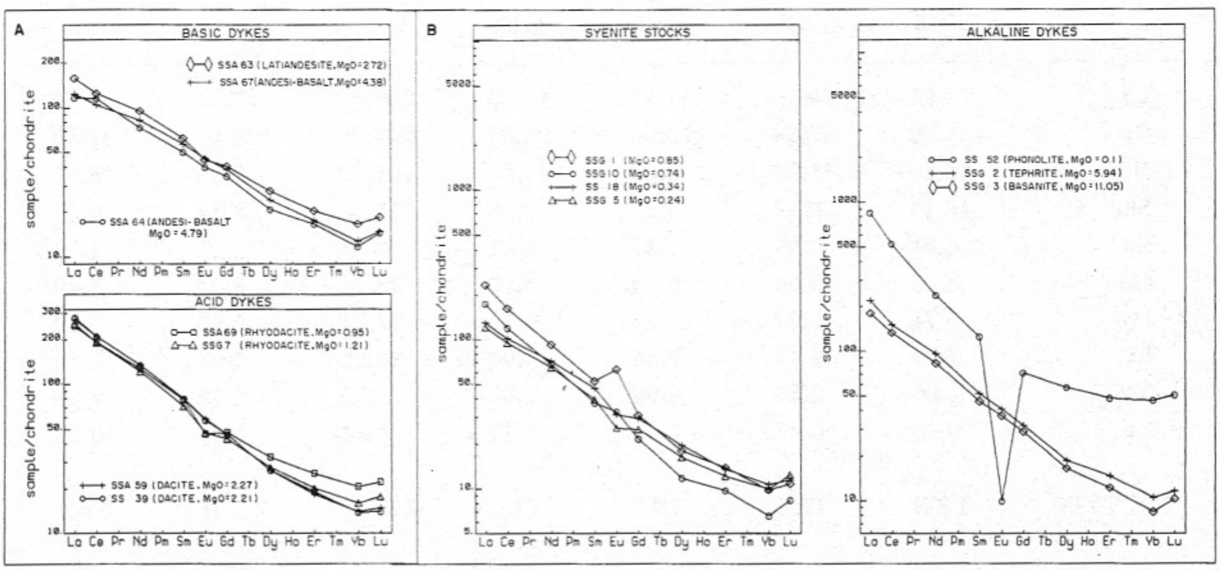

Figure 9 - REE patterns for the Early (A) and Late (B) Cretaceous magmatism from São Sebastião island. Chondrite-normalized according Boynton (1984).

Table 6. Rare earth elements (REE) analyses for Early and Late Cretaceous magmatic rocks from São Sebastião island. ICP analyses. Abbreviations as in Table 1.

SAMPLE	1 SS 39 D	4 SSA 59 D	6 SSA 63 D	7 SSA 64 D	10 SSA 67 D	13 SSG 7 D	15 SSA 69 D
La	87.03	84.85	48.88	36.39	38.24	78.94	76.28
Ce	169.10	168.87	101.19	94.03	84.40	154.37	155.69
Nd	80.10	80.41	56.91	44.02	49.59	73.24	75.38
Sm	15.48	15.62	12.13	9.77	11.13	13.81	15.23
Eu	4.24	4.32	3.29	2.92	3.33	3.46	3.41
Gd	11.97	11.95	10.46	9.00	9.93	11.23	12.40
Dy	8.53	8.57	8.95	6.75	7.74	9.01	10.49
Er	3.99	3.87	4.29	3.50	3.73	4.26	5.31
Yb	2.90	2.91	3.49	2.46	2.67	3.33	4.32
Lu	0.45	0.48	0.60	0.47	0.48	0.57	0.71
R. TYPE	DAC	DAC	LAND	AB	AB	RD	RD
La_N/Yb_N	20.20	19.70	9.40	10.00	9.70	16.00	11.90
Eu/Eu*	0.92	0.93	0.87	0.94	0.95	0.82	0.74

SAMPLE	22 SSG 1 S SERR	25 SS 18 S SSEB	27 SSG 5 S SSEB	28 SSG 10 S MIR	30 SS 52 D	34 SSG 2 D	35 SSG 3 D
La	72.41	40.15	37.85	54.06	263.65	67.91	55.80
Ce	131.70	82.34	76.66	96.81	424.20	122.00	107.93
Nd	55.10	43.24	38.91	41.01	142.52	57.59	49.47
Sm	10.18	9.17	7.73	7.30	24.32	10.11	9.03
Eu	4.65	2.29	1.87	2.41	0.73	3.02	2.71
Gd	8.05	7.64	6.48	5.60	18.54	8.24	7.49
Dy	5.78	6.29	5.25	3.81	18.31	6.03	5.30
Er	2.93	2.83	2.56	2.04	10.19	3.08	2.56
Yb	2.06	2.24	2.09	1.37	9.82	2.18	1.75
Lu	0.35	0.37	0.40	0.27	1.64	0.37	0.33
R. TYPE	TRC	TRC	TRC	TRC	PHON	TEPH	BAS
La_N/Yb_N	23.70	12.10	12.20	26.60	18.10	21.00	21.50
Eu/Eu*	1.52	0.81	0.79	1.11	0.10	0.98	0.98

Early Cretaceous dykes of the São Sebastião island (SSI) is the existence of a basic-acid magmatism whose bimodal character is similar to that of the Paraná flood volcanism (Bellieni et al., 1986; Piccirillo et al., 1988). It is worthwile mentioning that SSI-acid dykes chemically correspond (Bellieni et al., 1986) to the acid volcanics of northern Paraná (Chapecó type), which are enriched in incompatible elements. Note that this acid magmatism is very different from that of southern Paraná, characterized by low incompatible element contents (Palmas type). Moreover, as found for the northern Paraná volcanics, SSI-dacites and rhyodacites are closely associated with basalt types which are enriched in TiO_2 and incompatible elements. In general, geochemistry and mineral chemistry suggest that SSI-basic and acid dykes correspond to those of the Santos-Rio de Janeiro swarm, and therefore they can be considered as an easterly extension of this dyke swarm (Comin-Chiaramonti et al., 1983; Bellieni et al., unpublished data).

The *Late Cretaceous* SSI-magmatism is represented by syenite intrusions, and crosscutting alkaline dykes. These two distinct groups of alkaline rock types are characterized by different R_0 values: syenites = av. 0.7052, and basanite + tephrite = av. 0.7045. These isotope data clearly indicate that these two groups of alkaline rocks are related to different time-integrated mantle source materials. It is notable that syenitic stocks have very similar R_0 values. This support the possibility shown by geochemistry that the magma-type of São Sebastião stock can be derived from the less evolved syenitic magma-type of Serraria stock through fractional crystallization.

In the spidergram of Fig. 10, the EC tholeiitic SSI-dykes show La/Nb ratios higher than 1.0, and negative Nb-anomaly. On the contrary, the basanitic-tephritic rock-types of Late Cretaceous age have a distinct positive Nb-anomaly. On the whole, geochemistry and Sr-isotope data suggest that São Sebastião magmatism may be related to subcontinental lithospheric mantle.

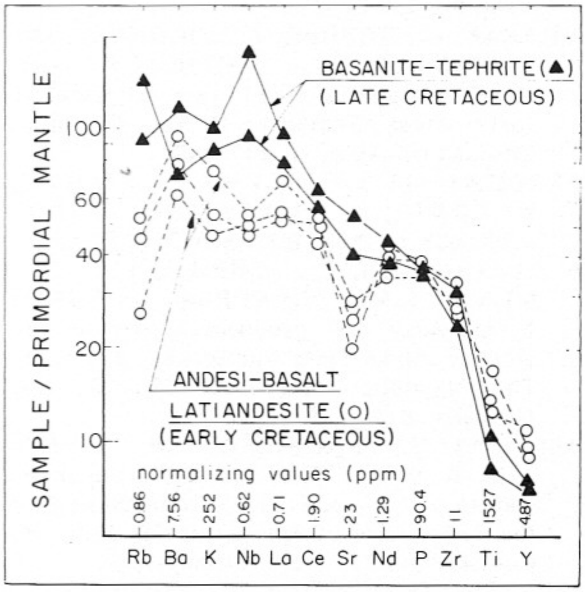

Figure 10 – Trace element abundances, normalized to primordial mantle values for Early and Late Cretaceous dykes from São Sebastião island.

ACKNOWLEDGEMENTS

The authors have benefitted from the financial support of CNPq, FAPESP, FINEP (Brazilian agencies), CNR and MURST (Italian agencies). The authors greatly benefitted from critical review and helpful suggestions of A. Cundari. They wish to express special thanks to L.S. Marques for help in the rare earth data treatment and to G. Mezzacasa, A. Giaretta, G. Rizzieri (CNR, Padova), as well as R. Zettin (Trieste University) for their collaboration in the technical and analytical work. IGC Project 257.

REFERENCES

ALMEIDA, F.F.M. (1986) Distribuição regional e relações tectônicas do magmatismo Pós-Paleozóico no Brasil. Rev. Bras. Geoc., **16**(4): 325-349.

AMARAL, G.; CORDANI, U.G.; KAWASHITA, K.; REYNOLDS, J.H. (1966) Potassium-argon dates of basaltic rocks from Southern Brazil. Geochim. Cosmochim.

Acta, **30**: 159-189.

AMARAL, G.; BUSHEE, J.; CORDANI, U.G.; KAWASHITA, K.; REYNOLDS, J.H. (1967) Potassium-argon ages of alkaline rocks from Southern Brazil. Geochim. Cosmochim. Acta, **31**: 117-142.

BARBIERI, M.; BECCALUVA, L.; BROTZU, P.; CONTE, A.; GARBARINO, C.; GOMES, C.B.; LOSS, E.L.; MACCIOTTA, G.; MORBIDELLI, L.; SCHEIBE, L.F.; TAMURA, R.M.; TRAVERSA, G. (1987) Petrological and geochemical studies of alkaline rocks from continental Brazil. 1. The phonolite suite from Piratini, RS. Geochim. Brasil., **1**: 109-138.

BELLIENI, G.; PICCIRILLO, E.M.; ZANETTIN, B. (1981) Classification and nomenclature of basalts. IUGS Subcommission on the systematics of igneous rocks. Circ. 34, Contribution 87, p. 1-19, Cambridge.

BELLIENI, G.; BROTZU, P.; COMIN-CHIARAMONTI, P.; ERNESTO, M.; MELFI, A.J.; PACCA, I.G.; PICCIRILLO, E.M.; STOLFA, D. (1983) Petrological and paleomagnetic data on the plateau basalts to rhyolite sequences of the Southern Paraná basin (Brazil). An. Acad. brasil. Ciênc., **55**: 355-383.

BELLIENI, G., COMIN-CHIARAMONTI, P., MARQUES, L.S., MELFI, A.J., NARDY, A.J.R., PAPATRECHAS, C., PICCIRILLO, E.M., ROISENBERG, A. & STOLFA, D. (1986) Petrogenetic aspects of acid and basaltic lavas from Paraná plateau (Brazil): geological, mineralogical and petrological relationships. J. Petrol., **27**: 915-944.

BELLIENI, G.; PICCIRILLO, E.M.; COMIN-CHIARAMONTI, P.; MELFI, A.J.; DA ROIT, P. (1988) Mineral chemistry of continental stratoid volcanics and related intrusives from the Paraná basin (Brazil). In: E.M. Piccirillo & A.J. Melfi (Eds.), The Mesozoic Flood Volcanism of the Paraná Basin: Petrogenetic and Geophysical Aspects. Ed. IAG, University of São Paulo, p. 73-92.

BOYTON, W.V. (1984) Cosmochemistry of the rare earth elements: meteorite studies. In: P. Henderson (Ed.), Rare Earth Element Geochemistry. Elsevier Publ. Co., Amsterdam, p. 63-114.

BUDDINGTON, A.F. & LINDSLEY, D.H. (1964) Iron-titanium oxide minerals and synthetic equivalents. J. Petrol., **5**: 310-357.

CARMICHAEL, I.S.E. (1967) The iron-titanium oxides of salic volcanic rocks and their ferro-magnesian silicates. Contr. Mineral. Petrol., **14**: 36-64.

COMIN-CHIARAMONTI, P.; GOMES, C.B.; PICCIRILLO, E.M.; RIVALENTI, G. (1983) High-TiO_2 basaltic dykes in the coastline of São Paulo and Rio de Janeiro states (Brazil). Neues. Jahr. Miner. Abh., **146**: 133-150.

DE LA ROCHE, H.; LETERRIER, J.; GRANDCLAUDE, P.; MARCHAL, M. (1980) A classification of volcanic and plutonic rocks using R_1-R_2 diagram and major-element analyses: its relationship with current nomenclature. Chem. Geol., **29**: 183-210.

ERNESTO, M. & PACCA, I.G. (1988) Paleomagnetism of the Paraná basin flood volcanics, Southern Brazil. In: E.M. Piccirilo & A.J. Melfi (Eds.), The Mesozoic Flood Volcanism of the Paraná Basin: Petrogenetic and Geophysical Aspects. Ed. IAG, University of São Paulo, p. 229-255.

ERNESTO, M.; PACCA, I.G.; HIODO, F.Y.; NARDY, A.J.R. (1990) Palaeomagnetism of the mesozoic Serra Geral Formation, Southern Brazil. Phys. Earth Planet. Int., **64**: 153-175.

FREITAS, R.O. (1947) Geologia e petrologia da Ilha de São Sebastião. Bol. FFCL/USP, 85, Geol. 3, 244p.

HENNIES, W.T. & HASUI, Y. (1968) Geocronologia das rochas eruptivas da Ilha de São Sebastião, SP. Anais XXII Congr. Bras. Geol., Belo Horizonte, 145-148.

HENNIES, W.T. & HASUI, Y. (1977) Contribuição ao reconhecimento da geologia da Ilha de Sao Sebastião. Simpósio de Geologia Regional, SBG, São Paulo, **1**: 199-209.

LEAKE, B.E. (1978) Nomenclature of amphiboles. Am. Mineral., **63**: 1023-1052.

MANTOVANI, M.S.M.; PEATE, D.W.; HAWKESWORTH, C.J. (1988) Geochemical stratigraphy of Paraná continental flood basalts: A contribution from borehole samples. In: E.M. Piccirillo & A.J. Melfi (Eds.), The Mesozoic Flood Volcanism of the Paraná Basin: Petrogenetic and Geophysical Aspects. Ed. IAG, University of São Paulo, p. 15-24.

MARQUES, L.S. (1988) Caracterização geoquímica das rochas vulcânicas da bacia do Paraná: Implicações petrogenéticas. Tese de doutoramento, IAG/USP, 175p.

MARQUES, L.S.; PICCIRILLO, E.M.; MELFI, A.J.; COMIN-CHIARAMONTI, P.; BELLIENI, G. (1989) Distribuição de terras raras e outros elementos traços em basaltos da bacia do Paraná (Brasil Meridional). Geochim. Brasil., **1**: 33-50.

MELFI, A.J. (1967) Potassium-argon dates for core samples of basaltic rocks from Southern Brazil. Geochim. Cosmochim. Acta, **31**: 1079-1089.

MELFI, A.J.; PICCIRILLO, E.M.; NARDY, A.J.R. (1988) Geological and magmatic aspects of the Paraná basin: An introduction. In: E.M. Piccirillo & A.J. Melfi (Eds.), The Mesozoic Flood Volcanism of the Paraná Basin: Petrogenetic and Geophysical Aspects. Ed. IAG, University of São Paulo, p. 1-13.

PAPIKE, J.J.; CAMERON, K.; BALDWIN, K. (1974) Amphiboles and pyroxenes: characterization of other than quadrilateral components and estimate of ferric iron from microprobe data. Bull. Geol. Soc. Amer., **6**: 1053-1054.

PETRINI, R.; CIVETTA, L.; PICCIRILLO, E.M.; BELLIENI, G.; COMIN-CHIARAMONTI, P.; MARQUES, L.S.; MELFI, A.J. (1987) Mantle heterogeneity and crustal contamination in the genesis of low-Ti continental flood basalts from the Paraná plateau (Brazil): Sr-Nd isotope and geochemical evidence. J. Petrol., **28**: 701-726.

PICCIRILLO, E.M.; COMIN-CHIARAMONTI, P.; MELFI, A.J.; STOLFA, D.; BELLIENI, G.; MARQUES, L.S.; GIARETTA, A.; NARDY, A.J.R.; PINESE, J.P.P.; RAPOSO, M.I.B.; ROISENBERG, A. (1988) Petrochemistry of continental flood basalt-rhyolite suites and related intrusives from the Paraná basin (Brazil). In: E.M. Piccirillo & A.J. Melfi (Eds.), The Mesozoic Flood Volcanism of the Paraná Basin: Petrogenetic and Geophysical Aspects. Ed. IAG, University of São Paulo, p. 107-156.

PICCIRILLO, E.M., BELLIENI, G.; CAVAZZINI, G.; COMIN-CHIARAMONTI, P.; PETRINI, R.; MELFI, A.J.; PINESE, J.P.P.; ZANTADESCHI, P.; DE MIN, A. (1990) Lower Cretaceous tholeiitic dyke swarms from the Ponta Grossa Arch (Southeast Brazil): Petrology, Sr-Nd isotopes and genetic relationships with the Paraná flood volcanics. Chem. Geol., **89**: 19-48.

RAPOSO, M.I.B. & ERNESTO, M. (1989) Rochas intrusivas básicas do Arco de Ponta Grossa: Resultados paleomagnéticos preliminares. Rev. Bras. Geoc., **19**(3): 393-400.

ROCHA-CAMPOS, A.C.; CORDANI, U.G.; KAWASHITA, K.; SONOKI, H.M.; SONOKI, I.K. (1988) Age of the Paraná flood volcanism. In: E.M. Piccirillo & A.J. Melfi (Eds.), The Mesozoic Flood Volcanism of the Paraná Basin: Petrogenetic and Geophysical Aspects. Ed. IAG, University of São Paulo, p. 25-45.

STEIGER, R.H. & JAEGER, E. (1977) Subcommission on geochronology: Convention on the use of decay constants in geo and cosmochronology. Earth Planet. Sci. Lett., **36**: 359-362.